Journal of Power Sources 186 (2009) 339–343

Contents lists available at ScienceDirect

Journal of Power Sources

journal homepage: www.elsevier.com/locate/jpowsour

Short communication

Self-assembly of palladium nanoparticles on functional multi-walled carbon nanotubes for formaldehyde oxidation

Zan-Zan Zhu [a], Zhe Wang [b,*], Hu-Lin Li [a,**]

[a] College of Chemistry and Chemical Engineering, Lanzhou University, Tianshui Road 222, Lanzhou 730000, China
[b] Mechanical and Aerospace Engineering Department, University of California Los Angeles, Los Angeles, CA 90095, United States

ARTICLE INFO

Article history:
Received 25 July 2008
Received in revised form 2 October 2008
Accepted 2 October 2008
Available online 11 October 2008

Keywords:
MWNTs
Palladium nanoparticles
Functionalization
Formaldehyde electrooxidation

ABSTRACT

In this work, we report a concise method to self-assemble Pd nanoparticles onto the surface of MWNTs. Highly dispersed palladium nanoparticles are loaded on the MWNTs functionalized with mercaptobenzene moieties. The structure of the resulting Pd–fMWNT composite were characterized by transmission electron microscopy (TEM), the results show that the chemically synthesized Pd nanoparticles were homogeneously dispersed and well-separated from one another on the functional MWNT surfaces. Cyclic voltammogram (CV) showed that Pd–fMWNT composite materials perform excellent electrocatalytic activity and long-term stability toward formaldehyde oxidation. Electrochemical impedance spectroscopy (EIS) revealed the strong interaction between fMWNTs and Pd facilitates the effective degree of electron dolocalization, and thus enhances the conductivity of the composite. The results imply that the self-organized Pd–fMWNT composite as a promising support material shows the excellent electrocatalytic activity and has a promising application potential in fuel cells and biosensors.

1. Introduction

Carbon nanotubes (CNTs) have captured the attention of researchers worldwide due to their unique nanostructures, remarkable electrical and mechanical properties [1–10]. In recent years, considerable efforts have been devoted to anchor noble metal particles onto the framework of carbon nanotube for their application in the area of catalysis. Some metals and their compounds, such as Pt, Pd, Ag, Au, Ni, Fe, Pt–Pd alloy have been deposited on the CNTs successfully [11–16]. CNTs were used as a potential support material for heterogeneous catalysts [17–19].

However, realistic applications have been hindered by difficulties associated with processing. Metal nanoparticles are spontaneously formed at the defect sites on the surface not on sidewall of carbon nanotubes. Simple deposition of metal nanoparticles on pristine CNTs leads to poor dispersion and bad stability. Therefore to obtain the good highly dispersed nanoparticles, the surface carbon nanotubes must be modified via a proper functionalization [20]. Generally speaking, this may be done either by covalent [8,21,22] or by noncovalent [23–26] sidewall functionalization. Recently Kim et al. [27] proposed a so-called atom-to-cluster (SAC) approach, which entails the deposition of an atomic layer of Pt atoms on thiolated (–SH functionalized) MWNTs. Chemical functionalization of carbon nanotubes with organic molecules might lead to new opportunities to anchor Pd nanoparticles onto the surface of MWNTs.

In this work, we demonstrate that Pd nanoparticles can self-assemble on MWNTs at very high surface densities. We functionalized the MWNTs via the diazotization reaction [28], and then deposited Pd nanoparticles onto the CNT surface by the aqueous solution reduction. The electrocatalytic activity of the product for formaldehyde oxidation was also investigated in detail. The procedure for the preparation of Pd-modified MWNT composite was shown in Fig. 1. This strategy not only could increase the number of surface nucleation sites for the nanoparticles but also could provide sufficient adhesion to prevent their diffusion along the CNT surface. The mercaptobenzene moieties are modified on the surface of MWNTs via a C–C covalent bond which is strong and propitious to anchor Pd nanoparticles onto them. Specially, this chemical process in the solution without sonication is suitable for production in industry.

2. Experimental

2.1. Preparation of functional MWNT (fMWNT)

MWNTs used in this work were produced via the chemical vapor deposition method, and their purity was about 95%. The process of

* Corresponding author. Tel.: +01 310 206 4501; fax: +01 310 206 4832.
** Corresponding author. Tel.: +86 931 891 2517; fax: +86 931 891 2582.
E-mail addresses: zhewang188@gmail.com, zhwang@ucla.edu (Z. Wang), lihl@lzu.edu.cn (H.-L. Li).

0378-7753/$ – see front matter © 2008 Elsevier B.V. All rights reserved.
doi:10.1016/j.jpowsour.2008.10.006

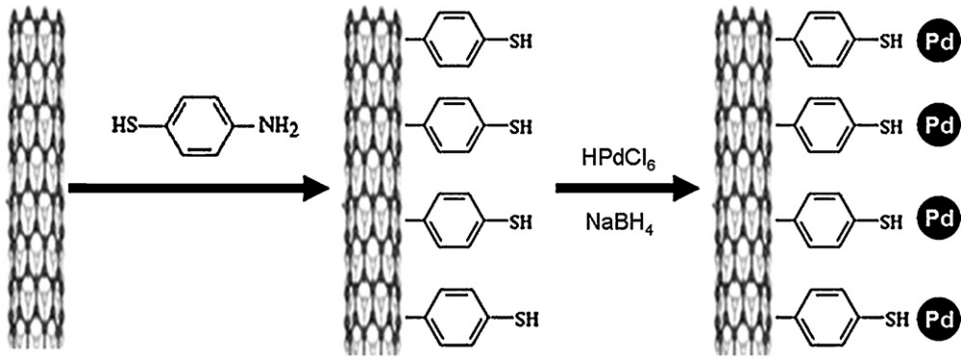

Fig. 1. Schematic illustration of the synthesis procedure of the composite.

preparation and purification are described in detail elsewhere [28]. 16 mg of MWNTs were devoted into 20 ml 1,2-dichlorobenzene (ODCB) under sonication for 10 min. The suspension was added to a solution of the 0.72 g 4-aminothiophenol in 10 ml acetonitrile, then bubbled with nitrogen for 10 min. After that, 1.71 ml isoamyl nitrite was quickly added via syringe. The mixed suspension was vigorous magnetic stirred at 60 °C for 24 h in an inert atmosphere. After cooling to room temperature, the suspension was diluted with dimethylformamide (DMF), filtered with a PTFE membrane disc filter (0.45 μm pore size) under vacuum followed by washing extensively with DMF until the filtrate became colorless [29]. Excess unreacted 4-aminothiophenol and isoamyl nitrite must be removed efficiently. DMF were removed by washing with sufficient absolute ethanol. Then, the MWNTs functionalized with mercaptobenzene moieties were obtained, which was denoted by fMWNT.

2.2. Preparation of Pd–fMWNT composite materials

The fMWNT were suspended in 10 ml ethanol with magnetic stirring. After that, 10 mg $PdCl_2$ is dissolved in acidified water (5 ml 0.05 M HCl), and this solution was added to the suspension so that it had the desired Pd loading. Then liquid ammonia was added to adjust the pH of the solution to about 8. Next, slow addition of 15 ml formaldehyde (37%) via syringe, keeping 20 °C and vigorous magnetic stirring. After 20 h, the solid was filtered and washed with deionized water for neutralization and then dried at 60 °C for 6 h in a vacuum oven. For comparison, Pd nanocatalyst supported on Vulcan-72 (Pd–C) was prepared under the same preparation conditions.

2.3. Preparation of Pd–fMWNT catalyst electrode

Five milligrams of Pd–fMWNT catalyst, 50 μL of Nafion solution (5 wt.%, Aldrich) and 1.0 ml of alcohol were mixed. A measured volume (ca. 25 μL) of this mixture was transferred via a syringe onto a glassy carbon electrode and heated under an infrared lamp to remove the solvent. The Pd–C catalyst electrode was also prepared under the same conditions.

2.4. Measurements

A conventional cell with a three-electrode configuration was used throughout this work. The working electrode was a Pd–fMWNT/GCE (glassy carbon electrode). A platinum sheet and a saturated calomel electrode (SCE) were used as counter and reference electrode, respectively. All electrochemical measurements were performed at room temperature using a CHI660A electrochemical working station (Covarda) controlled by CH instrument electrochemical software.

FTIR spectra were collected using a Nicolet Nexus 670 Fourier transform infrared spectrometer. The morphology of synthesized nanoparticles was observed on a Hitachi 600 transmission electron microscopy (TEM). The samples were prepared by dipping the Pd–fMWNT ethanol solution on the Cu grids and observed at 100 kV.

3. Result and discussion

3.1. FTIR analysis

Fig. 2. shows FTIR spectrum of (a) 4-aminothiophenol, (b) pristine MWNTs and (c) the MWNTs functionalized with mercaptobenzene moieties. By comparing with infrared spectra of curves (a) and (b), the peaks centered at 1622 and 1588 cm^{-1} are due to C—C stretching vibration of the benzene rings that attached to the framework of individual MWNT. The peaks centered at 1455 and 1487 cm^{-1} are related to the mixed C—C stretching and C—H bending vibration of benzene rings. The peak centered at 816 cm^{-1} is a well-known C—H out-of-plane bending vibration in paradisubstituted benzene. All mentioned peaks could be attributed to the presence of mercatophene moieties attached to the MWNTs [30].

3.2. TEM analysis

The surface morphology of Pd–fMWNT composite materials can be explored by TEM. It is well known that the MWNTs prepared by the chemical vapor deposition method are accompanied with many metal catalysts, support materials and amorphous carbon. There-

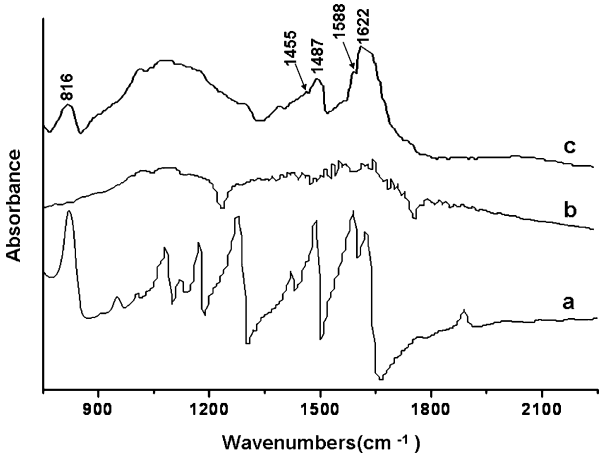

Fig. 2. FTIR spectrum of (a) 4-aminothiophenol, (b) pristine MWNTs and (c) the MWNTs functionalized with mercaptobenzene moieties.

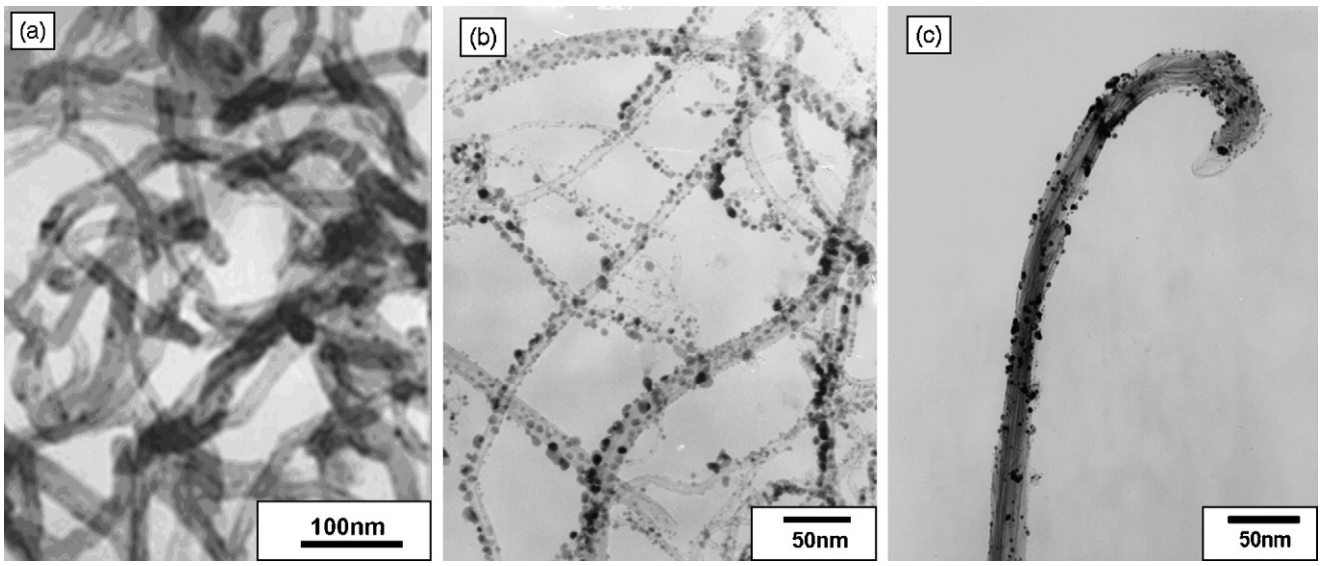

Fig. 3. Transmission electron micrograph (TEM) images of (a) MWNTs, (b) and (c) Pd–fMWNT composite materials.

fore, it is necessary to purify and functionalize the raw MWNTs to ensure the Pd particles are well deposited onto the MWNTs. Fig. 3a presents a typical TEM image of the MWNTs, showing a very clean surface for all the tubes, the diameters are in the range of 15–20 nm. The direct evidence of the formation of Pd nanoparticles on the surface of fMWNTs was given by Fig. 3b and c. It can be seen from Fig. 3b that well-dispersed, spherical particles are anchored onto the external walls of fMWNTs in large area. And the surface of fMWNTs was uniformly covered with a certain amount of palladium nanoparticles with an average size of 3–7 nm. Clearly, Fig. 3c shows that although Pd nanoparticles are distributed on fMWNTs with a quite high density, they do not aggregate with each other. This may because we protect fMWNTs surfaces through molecule-level design. Covalent bonding of the mercaptobenzene moieties on fMWNTs surfaces provides a uniform surface with positively charged sites which effectively isolate adjacent Pd nanoparticles [31].

3.3. Electrocatalytic activity towards formaldehyde

The CV curves of formaldehyde oxidation at the surface of (a) Pd–C and (b) Pd–fMWNT modified glassy carbon electrodes in the solution of 0.3 M HCHO + 0.1 M NaOH are presented in Fig. 4. CV was carried out in the potential window from +0.1 V to +1.0 V at the rate of 50 mV s^{-1}. Compared to curve (a), the most visible differences found for curve (b) are a lower peak potential and a higher peak current density. These contributed from the higher active surface area. At the same time, the onset potentials for formaldehyde oxidation on Pd–C is about 0.4 V. In contrast, the onset potential of formaldehyde electrooxidation on Pd–fMWNT occurs much earlier, at about +0.32 V. This indicates that the Pd–fMWNT catalyst is able to reduce significantly the overpotential in formaldehyde oxidation. In the anodic sweep of curve (b), the well-defined anodic peak at approximately +0.67 V (versus SCE) is attributable to the oxidation of CO to CO_2 [32]. In the reverse sweep, another anodic peak is observed at approximately +0.50 V (versus SCE) due to the complete oxidation of HCHO to CO_2 via a dehydrogenation reaction ($HCHO + H_2O - CO_2 + 4H^+ + 4e$). Additionally, the ratio of peak current associated with the anodic peaks in the forward (I_f) and reverse (I_b) scans is used to infer the CO tolerance of the catalysts [33]. A lower I_f/I_b value indicates poor oxidation of formaldehyde to CO during the anodic scan and excessive accumulation of residual carbon species on the catalyst surface, in other words, a greater extent of CO poisoning. Hence a higher I_f/I_b value is indicative of improved CO tolerance. From Fig. 4, the I_f/I_b ratio of 1.34 for Pd–fMWNT electrode is higher than that of Pd–C ($I_f/I_b = 1.28$), which indicated more intermediate carbonaceous species are oxidized to carbon dioxide in the forward scan on Pd–fMWNT electrode surface than on Pd–C. These differences demonstrate that for Pd–fMWNT composite materials the kinetics of the formaldehyde oxidation is tremendously improved and the oxidation of HCHO becomes much easier [34]. Therefore, Pd–fMWNT composite materials have a higher electrocatalytic activity in the formaldehyde oxidation reaction. This might be attributed to the high dispersion and the effective adhesion of Pd nanoparticles on fMWNTs. Meanwhile, Pd–fMWNT composite materials have highly active surface area will have more active sites for electrochemical reaction than Pd–C composite materials. Therefore, the fMWNTs as a support of Pd-based electrocatalyst for formaldehyde oxidation shows a better performance than that of Vulcan-72 support, thereby proving to be an efficient catalyst support, which appears as a promising field of research.

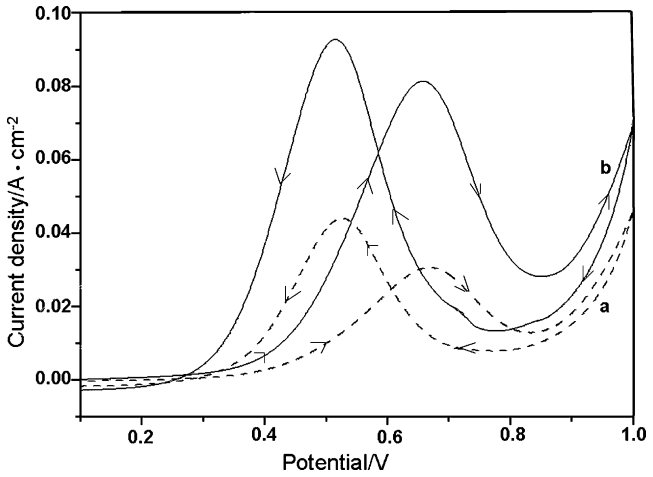

Fig. 4. The potential cyclic voltammogram of electrooxidation of formaldehyde oxidation in alkaline solutions (0.3 M HCHO in 0.1 M NaOH) at GCE with (a) Pd–C and (b) Pd–fMWNT (vs. SCE).

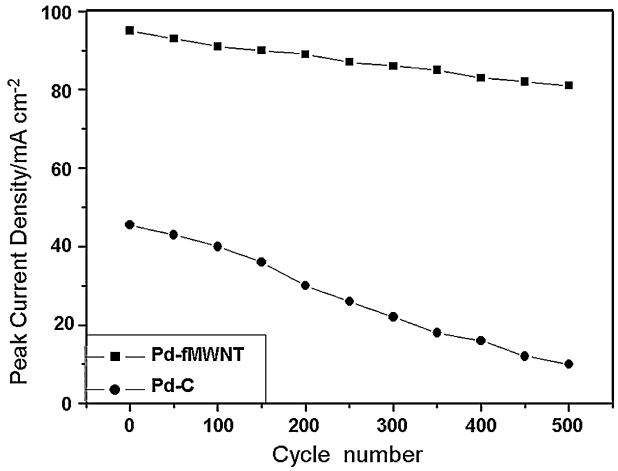

Fig. 5. Long-term stability of the electrodes in 0.3 M HCHO in 0.1 M NaOH (scan rate: 50 mV s^{-1}).

3.4. Long-term stability towards formaldehyde

The long-term stability of the Pd–fMWNT composite materials was also investigated in 0.3 M HCHO + 0.1 M NaOH solution. For reference, Pd–C catalyst was also chosen in this experiment, and the results were shown by Fig. 5. It can be observed that both the peak currents of Pd–fMWNT and Pd–C composites decrease gradually with the successive scans. Comparing two curves, the Pd–fMWNT composite in our experiment still have excellent stability in alkaline solution after the long-term CV experiment. This indicates that the Pd–fMWNT composite prepared in our experiment has good durability and stability.

3.5. Electrochemical impedance spectroscopy analysis

Fig. 6. presents the impedance spectrum of the (a) Pd–fMWNT and (b) Pd–C composite materials, respectively. It can be seen that although fMWNTs had been incorporated into the composite, both of the impedance spectrums are almost similar in form, composed of a depressed semicircle at high frequencies and a linear spike at low frequencies. The high frequency intercept on real axis is due to solution resistance. At high frequencies, the diameter of the semicircle has been considered as the charge transfer resistance representing the rate of charge exchange between ions in aqueous and composite at electrochemical interface [35]. As well as in the low-frequency region the straight line can be attributed to Warburg impedance [36,37].

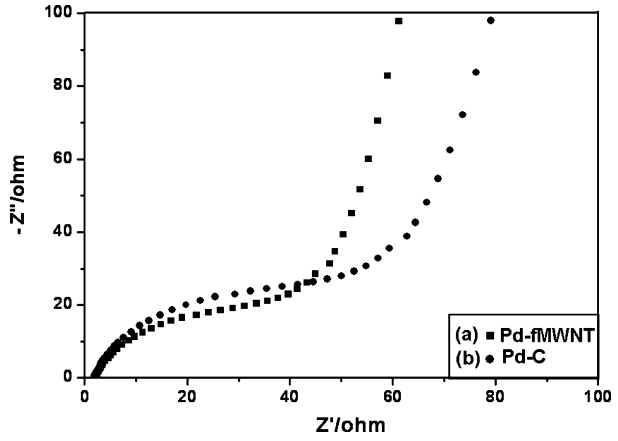

Fig. 6. Complex-plane impedance plots for the (a) Pd–fMWNT and (b) Pd–C composite materials.

In spite of the similar shape of the impedance spectra, there is an obvious difference between the diameters of the two semicircles. It can be seen that the diameter of the semicircle of (a) is smaller than that of (b). In other words, smaller charge-transfer resistance is found for Pd–fMWNT composite materials, indicating a smaller reaction resistance than Pd–C composite materials. This fact may suggest that the strong interaction between fMWNTs and Pd facilitates the effective degree of electron delocalization, and thus enhances the conductivity of the composite. Meanwhile, in low-frequency regions, the slope of (a) was higher than (b). This displays that the application of fMWNTs as supporting materials helps to promote mass diffusion. The above results also suggest that dispersed Pd nanoparticles on fMWNTs may make the composite materials have the higher catalytic activity for formaldehyde oxidation. It is consistent with the result of CVs.

4. Conclusions

A concise method to self-assemble Pd nanoparticles onto the surface of MWNTs has been reported in this work. Highly dispersed palladium nanoparticles are loaded by the aqueous solution reduction on mercaptobenzene moieties grafted MWNTs. The dispersion and electrocatalytic properties of palladium on the MWNTs have also been investigated. The Pd–fMWNT composite material shows excellent electrocatalytic activity for formaldehyde oxidation and long-term cycle stability. This may be attributed to the high dispersion of nanoscale palladium catalysts and the specific and complex nature of functional MWNTs. This technique is not limited to Pd, it may be used to prepare a variety of metal nanoparticles on MWNTs surfaces for catalysis applications. In view of the advantage of industry and environmentally benign nature of the material, this method is believed to have a great potential for large-scale applications.

Acknowledgement

This work was supported by the National Natural Science Foundation of China (Grant No. 60471014).

References

[1] T.W. Ebbesen, H.J. Lezec, H. Hiura, J.W. Bennett, H.F. Ghaemi, T. Thio, Nature 382 (1996) 54.
[2] E.W. Wong, P.E. Sheehan, C.M. Lieber, Science 277 (1997 1971).
[3] P. Poncharal, Z.L. Wang, D. Ugarte, W.A. de Her, Science 283 (1999) 1513.
[4] Z. Liu, X. Lin, J.Y. Lee, W. Zhang, M. Han, L.M. Gan, Langmuir 18 (2002) 4054.
[5] H. Dai, J.H. Hafner, A.G. Rinzler, D.T. Colbert, R. Smalley, Nature 384 (1996) 147.
[6] B.I. Yakobson, R.E. Smalley, Am. Sci. 85 (1997) 324.
[7] P. Calvert, Nature 399 (1999) 210.
[8] C.A. Dyke, J.M. Tour, J. Phys. Chem. A 108 (2004) 11151.
[9] Z. Wang, M. Lu, H.L. Li, X.Y. Guo, Mater. Chem. Phys. 100 (2006) 77.
[10] M.S. Dresselhaus, G. Dresselhaus, P. Avouris, Top. Appl. Phys. 80 (2001) 1.
[11] G.G. Wildgoose, C.E. Banks, R.G. Compton, Small 2 (2006) 182.
[12] X.H. Chen, J.T. Xia, J.C. Peng, W.Z. Li, S.S. Xie, Compos. Sci. Technol. 60 (2000) 301.
[13] B. Yoon, C.M. Wai, J. Am. Chem. Soc. 127 (2005) 17174.
[14] L.M. Ang, T.S.A. Hor, G.Q. Xu, C.H. Tung, S.P. Zhao, J.L.S. Wang, Carbon 38 (2000) 363.
[15] F.Z. Kong, X.B. Zhang, W.Q. Xiong, E. Liu, W.Z. Huang, Y.L. Sun, J.P. Tu, X.W. Chen, Surf. Coat. Technol. 155 (2002) 33.
[16] X. Hu, T. Wang, X. Qu, S. Dong, J. Phys. Chem. B 110 (2006) 853.
[17] J.M. Planeix, N. Coustel, B. Coq, V. Brotons, P.S. Kumbhar, R. Dutartre, P. Geneste, P. Bernier, P.M. Ajayan, J. Am. Chem. Soc. 116 (1994) 7935.
[18] C. Pham-Huu, N. Keller, M.J. Ledoux, L.J. Charbonniere, R. Ziessel, Chem. Commun. 19 (2000 1871).
[19] C.H. Liang, Z.L. Li, J.S. Qiu, C. Li, J. Catal. 211 (2002) 278.
[20] D.J. Guo, H.L. Li, Carbon 1259 (2005) 43.
[21] Y. Ying, R.K. Saini, F. Liang, A.K. Sadana, W.E. Billups, Org. Lett. 5 (2003) 1471.

[22] P.J. Boul, J. Liu, E.T. Mickelson, C.B. Huffman, L.M. Ericson, I.W. Chiang, K.A. Smith, D.T. Colbert, R.H. Hauge, J.L. Margrave, R.E. Smalley, Chem. Phys. Lett. 310 (1999) 367.
[23] M.J. O'Connell, P.J. Boul, L.M. Ericson, C.B. Huffman, Y. Huang, E.H. Haroz, K.D. Ausman, R.E. Smalley, Chem. Phys. Lett. 342 (2001) 265.
[24] A. Star, J.F. Stoddart, D. Steuerman, M. Diehl, A. Boukai, E.W. Wong, X. Yang, S.W. Chung, H. Choi, J.R. Heath, Angew. Chem. 113 (2001 1721).
[25] R.J. Chen, Y. Zhang, D. Wang, H. Dai, J. Am. Chem. Soc. 123 (2001) 3838.
[26] A.B. Dalton, C. Stephan, J.N. Coleman, B. McCarthy, P.M. Ajayan, S. Lefrant, P. Bernier, W.J. Blau, H.J. Byrne, J. Phys. Chem. B 104 (2000) 10012.
[27] Y.T. Kim, K. Ohshima, K. Higashumine, T. Uruga, M. Takata, H. Suematsu, T. Mitani, Angew. Chem. Int. Ed. 45 (2006) 407.
[28] J.L. Bahr, J.M. Tour, Chem. Mater. 13 (2001) 3823.
[29] C.A. Dyke, J.M. Tour, J. Am. Chem. Soc. 125 (2003) 1156.
[30] J. Shi, Z. Wang, H.L. Li, J. Nanopart. Res. 8 (2006) 743.
[31] G.W. Yang, G.Y. Gao, G.Y. Zhao, H.L. Li, Carbon 45 (2007) 3036.
[32] L.H. Mascaro, D. Goncalves, L.O.S. Bulhoes, Thin Solid Films 461 (2004) 243.
[33] Z.L. Liu, X.Y. Ling, X.D. Su, J.Y. Lee, J. Phys. Chem. B 108 (2004) 8234.
[34] H.T. Zheng, Y.L. Li, S.X. Chen, P.K. Shen, J. Power Sources 163 (2006) 371.
[35] G. Wu, L. Li, J.H. Li, B.Q. Xu, J. Power Sources 155 (2006) 118.
[36] Z. Wang, Z.Z. Zhu, J. Shi, H.L. Li, Appl. Surf. Sci. 253 (2007) 8811.
[37] A. Tarola, D. Dini, E. Salatelli, F. Andreani, F. Decker, Electrochim. Acta 44 (1999) 4189.